Underwater Heritage documentation using photogrammetry: the CRAB system

Underwater Heritage documentation using photogrammetry: the CRAB system

Beatrice Tanduo [1], Edward Borgogno [1], Filiberto Chiabrando [1], Francesca Gallitto [2] , Stefania Manca [2], Paolo Maschio [2], Andrea Lingua [2]

[1] Laboratory of Geomatics for Cultural Heritage (LabG4CH), Department of Architecture and Design (DAD), Politecnico di Torino, Viale Pier Andrea Mattioli, 39, Torino (TO), Italy – (beatrice.tanduo; edward.borgogno; filiberto.chiabrando)@polito.it
[2] Geomatics Lab, Department of Environment, Land and Infrastructure Engineering (DIATI), Politecnico di Torino, Corso Duca degli Abruzzi, 24, Torino (TO), Italy – andrea.lingua@polito.it

Keywords: Underwater, Cultural Heritage, photogrammetry, submerged archaeology, 3D survey.

Abstract

The documentation and preservation of submerged cultural heritage present significant challenges due to the complexity of the underwater environment, including issues related to accessibility, visibility, and the lack of reliable reference data for scaling and orientation. This study introduces CRAB (Calibrated Rig for Aquatic photogrammetric Bicamera system), a stereoscopic imaging system designed to support high-resolution 3D reconstruction of underwater archaeological sites. The system integrates two synchronised, full-frame 60 MP cameras on a fixed baseline and employs dome ports with optically calibrated alignment to minimise refractive distortion. Field testing was conducted at a submerged Roman shipwreck site in the Marine Protected Area of Porto Cesareo, Italy, where five large "cipollino" marble columns were surveyed. Over 1300 stereoscopic image pairs were acquired using a structured acquisition pattern. Post-processing included camera calibration, colour correction, and 3D model reconstruction using a standardised SfM (Structure from Motion) approach. Results demonstrated that the CRAB system thus offers a reliable and scalable solution for accurate underwater photogrammetry and represents a valuable contribution to the documentation and conservation of submerged cultural assets.

1. Introduction

Submerged cultural heritage represents a valuable resource from an ecological, scientific, educational, and economic perspective. Therefore, it requires appropriate conservation and enhancement measures to continue providing significant benefits to the communities that engage with it.

The values of modern technologies and innovative methods used today for the documentation of heritage (Ricca et al., 2020; Violante et al,. 2023) is not only linked to the their ability to ease and facilitate knowledge sharing among experts and researchers, but also in their crucial role in engaging the wider public. In recent years, the use of virtual technologies has expanded well beyond the academic and scientific sphere. Many museums and marine protected areas (MPAs) have begun adopting 3D modelling and visualization tools not only for the scientific dissemination of research findings but also for historical interpretation and public outreach. These technologies allow broader audiences to access, explore, and appreciate underwater heritage through interactive experiences, immersive virtual reconstructions, and digital exhibitions, making cultural content more accessible and engaging than ever before.

The growing demand for high-resolution 3D products to support the conservation and enhancement of submerged archaeological sites has introduced a series of challenges in underwater surveying and monitoring. The difficulty in documenting such archaeological sites is primarily due to their location (both in position and depth) and their intrinsic vulnerability (Auriemma et al., 2021). Although many technological and methodological solutions for documenting archaeology using geomatic techniques are already available for terrestrial environments, the challenge remains open for the underwater context (Calantropio et al., 2021).

Underwater photogrammetry is an essential technique for underwater archaeology, allowing the creation of detailed three-dimensional models (Balletti et al., 2015; Calantropio and Chiabrando, 2024). However, the submerged environment presents significant challenges, including geometric distortions due to refraction, colour alterations caused by selective light absorption (Schettini and Corchs, 2010), and difficulties in acquiring ground control points, which are crucial for model orientation and scaling.

In addition to these well-known constraints, underwater imaging is further complicated by the dynamic nature of the marine environment, which includes variable turbidity, water column stratification, suspended particulate matter, and biological growth on surfaces. These factors limit visibility, reduce image contrast, and introduce non-uniform illumination, ultimately affecting the accuracy and reliability of photogrammetric outputs.

In response to these challenges, this study presents the design and validation of a new underwater stereophotogrammetric system developed within the framework of the ARCHIM3DES (ARchaeological and Cultural Heritage documentation In Marine environment using advanced 3D mEtric Survey techniques) and POSEIDON (multitemPOral SEagrass mapping and monitoring of posIDONia meadows and banquettes for blue carbon conservation) projects. The proposed system, named CRAB (Calibrated Rig for Aquatic photogrammetric Bicamera system), aims to provide a portable, scalable, and accurate solution for high-resolution 3D reconstruction of submerged cultural heritage. By employing a fixed stereo baseline, high-resolution synchronised imaging, and optically calibrated dome ports, CRAB seeks to overcome current limitations in underwater photogrammetric workflows and to enhance the reliability and precision of spatial data collected in submerged archaeological contexts.

2. System design and development

CRAB (Figure 1) consists of two Sony ILX-LR1 cameras with 60 MP full-frame sensors equipped with Sigma 17mm F4 DG

DN lenses. Each camera, capable of simultaneously capturing high-resolution stereoscopic pairs, is enclosed in an underwater housing (producer LEONE Sub) equipped with a glass dome port. It is also equipped with two lighting units, each delivering 21000 lumens (producer Easydive). The main specifications of the two cameras and lenses are reported in Table 1 and Table 2.

(a)

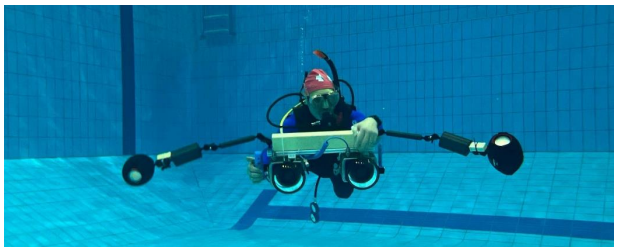

(b)

Figure 1. Current configuration of the CRAB system (a) and the system during a test in the pool (b).

	SONY ILX-LR1
Pixel size	3,8 µm
Sensor Type	CMOS Exmor R 35.7 x 23.8 mm
Images resolution	9504 x 6336 pixels
Weight	243 g
Dimensions (L x W x H)	100 x 42,5 x 74 mm

Table 1. Cameras Sony ILX-LR1 specifics (https://pro.sony/en_NO/products/installable-cameras/ilx-lr1)

	SIGMA 17mm F4 DG DN
Focal Length	17 mm
Weight	220 g
Dimensions (φ x L)	64 x 48,8 mm

Table 2. Lenses Sigma 17mm F4 DG DN specifics (https://www.sigma-global.com/en/lenses/c023_17_4/)

2.1 Cameras' synchronisation and trigger control

The synchronisation of the two cameras is managed by a microcontroller unit (MCU), which captures the electrical pulse generated by the trigger button on the external control unit. This pulse is induced by the displacement of a magnet, producing a low-voltage signal. The MCU, running custom firmware specifically developed for this application, interprets the input as a trigger event, amplifies the signal, and distributes it to both cameras via the internal electrical wiring integrated within the underwater housings. The microcontroller can handle multiple types of input, depending on the firmware uploaded. A dedicated firmware version has been developed to enable automatic multi-shot sequences. The shooting frequency can be configured in the source code and uploaded to the MCU according to the specific requirements of the survey or data acquisition task.

2.2 Architecture of CRAB

The cameras are protected by watertight anodised aluminium housings and are fixed together on a base, supporting lighting elements. The known fixed base of 350 mm between the two cameras allows scaling of the 3D model reconstructed by Structure From Motion algorithms without needing ground control points, which can be challenging to acquire at significant depths. Both cameras are equipped with glass dome ports, whose curvature centres have been determined to make them coincident with the position of the entrance pupil of the camera's lens (Menna et al., 2016).
To determine the radius of curvature of the dome ports, the glass elements have been opacified and their surfaces were scanned using the Mantis Vision F6 Short Range structured infrared light scanner. A spherical surface was then fitted to the resulting point cloud, allowing the estimation of the curvature centre (Figure 2).

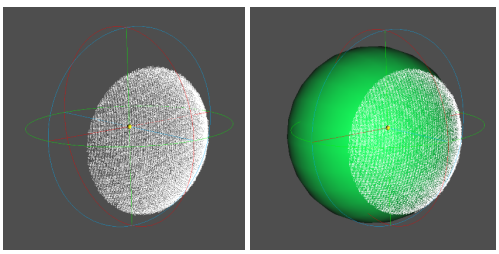

(a) (b)

Figure 2. The obtained point cloud of the dome port (a) and the computing process of the dome port curvature using the best fitting sphere (b). The so computed curvature radius is 88 mm.

The entire device has been made neutrally buoyant by adding a high-density polyurethane foam element fixed to the connecting bar between the two underwater housings. The volume of this element was calculated based on a density of 192 kg/m³ in order to counteract the weight force of the two housings alone, along with their contents and the connecting bar, when submerged in water. The lighting units are considered slightly positively buoyant in water and are used to stabilize the system in the desired acquisition configuration.

2.3 Centring and settings of the cameras

The alignment of the cameras' lenses with the centres of the domes has been verified following an empirical approach that consists, in a controlled environment, of positioning the camera half-submerged in water, capturing an image of a calibration panel also partially submerged (Figure 3). This ensured that both the above-water and underwater portions of the image were in focus and that the panel's vertical lines did not suffer from distortion (She et all., 2019, She et all., 2022).

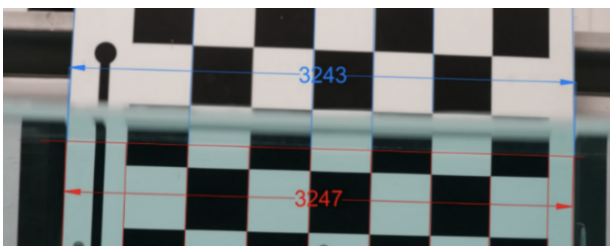

Figure 3. Image of the partially submerged calibration panel during the camera's centring verification test.

Both cameras have been set to aperture priority shooting mode with an aperture of f/9 and ISO 800. With these settings, the

cameras calculate the shutter speeds based on the lighting conditions. The tests have been conducted in an indoor pool with a maxim depth of 4 m with the system's built-in artificial lighting turned on (Figure 4). The resulting shutter speeds ranged from 1/80 to 1/320 of a second, depending on the object's acquisition distance.

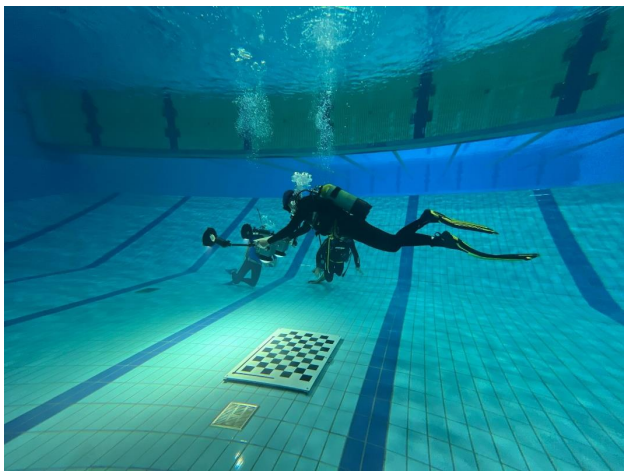

Figure 4. CRAB during a test in the pool.

These exposure times, obtained in controlled conditions simulating typical underwater lighting scenarios, are well-suited for handheld photogrammetric acquisition by a diver operating the CRAB system in real-world marine environments, ensuring sharp images without significant motion blur.
The comprehensive testing and calibration of the CRAB system, including camera synchronisation, optical alignment, and structural buoyancy adjustments, have demonstrated its reliability and precision for underwater photogrammetric data acquisition. With the technical setup validated, the next phase involved deploying the system in a real-world archaeological context to assess its performance in situ.

3. Survey campaign

The photogrammetric survey has been carried out as part of a coordinated field operation involving both the Geomatics team and the underwater archaeology team from Università del Salento. This close collaboration was fundamental to the success of the project, as it enabled an integrated approach that combined metric documentation expertise with archaeological support and site knowledge.
During the survey (July 2024), the archaeologists provided essential assistance during the operations, ensuring the safety of the site and facilitating access to the columns, speeding up and easing the documentation process. The columns, which are always partially exposed on the seabed, have been documented under natural conditions. The visibility of the full extent of the columns' surfaces significantly enhanced the quality and completeness of the 3D reconstruction.
The geomatics team participated directly in the underwater operations, diving alongside the archaeologists and coordinating the photogrammetric acquisition in alignment with optimal weather and sea conditions to ensure maximum water clarity and stability.
A structured acquisition protocol was adopted to guarantee full coverage of the archaeological site and to enhance the accuracy and completeness of the 3D reconstruction.

3.1 Case study

The system has been tested at a submerged archaeological site located in the Marine Protected Area (MPA) of Porto Cesareo, near Lecce, in southern Italy. Specifically, the test was conducted off the coast of Torre Chianca, where five large monolithic columns lie on the sandy seabed at a depth of approximately 4.5 meters and just 80 meters from the shoreline (Figure 5). These columns, dating back to the 2nd century AD, are the only remaining visible elements of a Roman shipwreck, discovered in 1960 and identified as a *navis lapidaria*, that sank while transporting a cargo of various artefacts and monumental architectural elements during a voyage that started from the island of Euboea in the Aegean Sea.
The columns, quarried in Karystos and made of "cipollino" marble, are between 9 meters long and 70 to 100 centimetres in diameter. Their surfaces remain in a roughly hewn state, with fluting only partially sketched out, indicating they were still unfinished at the time of transport. Today, the columns are largely covered by green algae and scattered marine life such as sponges, offering a unique combination of archaeological and biological interest.

(a) (b)

Figure 5. Porto Cesareo seashore, where both the tower (Torre Chianca) and the submerged columns can be seen (a) and CRAB during the acquisition phase (b).

3.2 Data acquisition

The data acquisition followed a traditional grid-based photogrammetric approach, wherein images were captured systematically along parallel transects at regular intervals. This method ensured consistent overlap between consecutive stereoscopic pairs, which is essential for robust feature matching during Structure-from-Motion (SfM) processing. Both nadiral (vertical) and oblique (approximately 45°) images have been acquired, to capture the geometry of the columns from multiple perspectives, improving the photogrammetric reconstruction of vertical and occluded surfaces. In addition to the grid acquisition, a radial acquisition scheme was implemented around the five columns to obtain dense image coverage of the curved and irregular features of the archaeological elements. This hybrid acquisition strategy allowed for detailed documentation of the entire site, including the morphology of the marble columns, their state of preservation, and their spatial arrangement on the seabed (Figure 6).

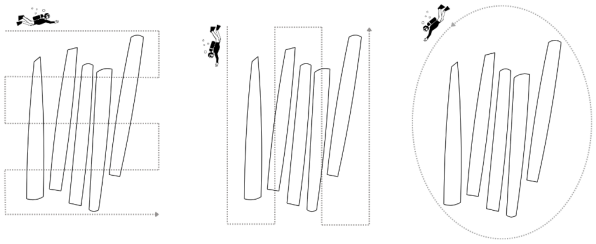

Figure 6. Schema of path followed during the data acquisition phase.

Throughout the campaign, the CRAB system operated at a consistent elevation above the seabed, maintaining a stable and controlled trajectory. This approach was crucial to minimise any disturbance to the sediment and to preserve the integrity of the underwater archaeological site. The stereo pairs have been acquired at high frequency, resulting in 2632 synchronized images (1316 stereo pairs) that collectively covered the full extent of the archaeological site and the surrounding context (Figure 7).

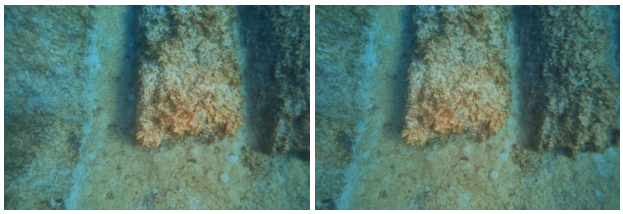

Figure 7. Example of a stereoscopic pair acquired by CRAB (Camera B on the left and Camera A on the right).

4. Data processing

The post-processing workflow involved three primary phases: internal camera calibration to refine the intrinsic parameters of the imaging system, radiometric normalization through colour correction techniques adapted to underwater conditions, and dense 3D reconstruction via a Structure-from-Motion (SfM) approach.

4.1 Camera calibration

This study employed a pre-calibration method using a 120x85 cm checkerboard panel.
The camera calibration has been carried out using Agisoft Metashape (version 2.0.3). The first step involved obtaining the calibration parameters by collimating, across 15 images, 88 markers, positioned at each corner of the checkerboard calibration panel (Figure 8).

Figure 8. The calibration panel on the seabed with the 88 markers detected by the Agisoft Metashape software.

The intrinsic parameters derived from this process include the focal length (f), principal point coordinates (cx, cy), and radial and tangential lens distortion coefficients (k1, k2, k3, k4 for radial, and p1, p2 for tangential). Additionally, parameters b1 and b2 account for affine distortions related to sensor geometry or mechanical misalignments. Together, these parameters define the internal geometry of the camera and describe how 3D points are projected onto the 2D image plane, accounting for optical imperfections introduced by the lens system.
These initial values serve as preliminary estimates for the subsequent self-calibration procedure conducted during the Bundle Block Adjustment (BBA) phase of the entire dataset processing, where further refinement is performed to optimize the photogrammetric solution.

4.2 Colour correction

The colour correction process, which has been done inside the MATLAB environment, is based on a regression-based correction model using a ColorChecker chart captured in the underwater scene. Various tests have been conducted on two images from the right and the left cameras, where the X-Rite ColorChecker (Figure 9) is clearly visible. The chart provides 24 colour reference patches with known target values in the Lab colour space, where L represents lightness of the colour, ranging typically from 0 (black) to 100 (white), the a component corresponds to colour positioning along the green-red axis, and The b component describes the position along the blue-yellow axis.

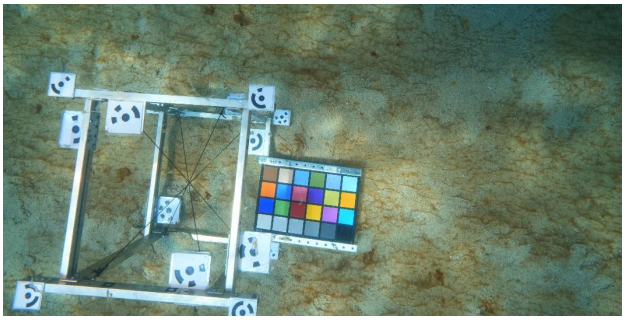

Figure 9. Original underwater image acquired with the ColorChecker positioned in the scene. This serves as the baseline for evaluating colour distortions before applying any correction.

First, each patch in the image is extracted and converted to Lab, and the colour difference (ΔE) between the measured and reference Lab values is computed. These ΔE values are computed as:

$$\Delta E = \sqrt{(L_1 - L_2)^2 + (a_1 - a_2)^2 + (b_1 - b_2)^2} \quad (1)$$

where ΔE = Euclidean distance between two colour points in the CIELAB colour space
L_1, a_1, b_1 = measured values
L_2, a_2, b_2 = reference values

The obtained values are used to assess the colour distortion introduced by the underwater environment quantitatively.
To visualise the extent of distortion, an image is generated in which each patch is displayed with its corresponding ΔE value overlaid (Figure 10). This provides a quick and interpretable way to evaluate colour accuracy. For instance, some patches such as Patch 7 (ΔE = 7.7) and Patch 16 (ΔE = 8.3) show low colour error, while others like Patch 10 (ΔE = 58.9) and Patch 13 (ΔE =

47.4) reveal substantial deviations, highlighting the non-uniform nature of underwater colour shifts.

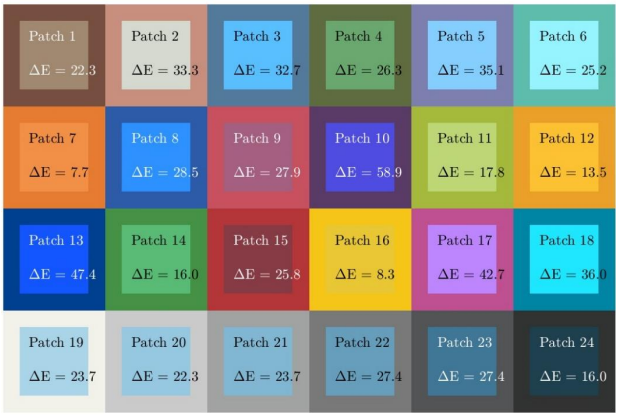

Figure 10. Visualization of the colour differences (ΔE) between the measured and reference ColorChecker patches before correction.

To correct these distortions, a second-order polynomial regression model is fitted using the measured and reference Lab values from the chart. Unlike simpler linear models, this method accounts for non-linear colour distortions by including both the original and squared terms of the Lab channels. Specifically, for each patch, two vectors are determined:
the input feature vector

$$X = [L^* a^* b^* (L^*)^2 (a^*)^2 (b^*)^2\ 1] \quad (2)$$

and the target output vector

$$Y = [\, L^*_{ref}\ \ a^*_{ref}\ \ b^*_{ref}] \quad (3)$$

The regression coefficients are computed through a weighted least-squares solution, where weights are inversely proportional to the ΔE values. This ensures that patches with greater discrepancies have more influence during the fitting process, leading to a more robust correction model.
Once trained, the model is applied pixel-wise to the entire image. The image is first converted to Lab and reshaped into a vector of pixels. Each pixel is then transformed using the learned regression matrix. The corrected Lab values are reshaped to the original image dimensions and converted back to RGB, with an optional gamma adjustment applied to refine the final visual output (Figure 11).

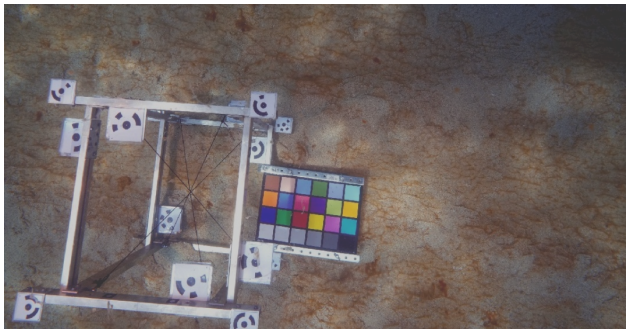

Figure 11. Corrected image after applying the colour correction model.

This polynomial regression-based approach allows for a more accurate correction of underwater colour distortions, improving chromatic fidelity by accounting for complex, non-linear behaviours in the imaging pipeline.
The calibration model has then been systematically applied to the complete stereoscopic dataset (Figure 12). This allowed for a consistent and optimised chromatic correction across all images, effectively compensating for underwater-specific distortions such as chromatic shifts due to refraction and selective light absorption.
The colour-corrected images have then been used to generate the photorealistic texture of the final 3D model, ensuring a visually coherent and perceptually accurate representation of the archaeological surfaces and materials.

(a)

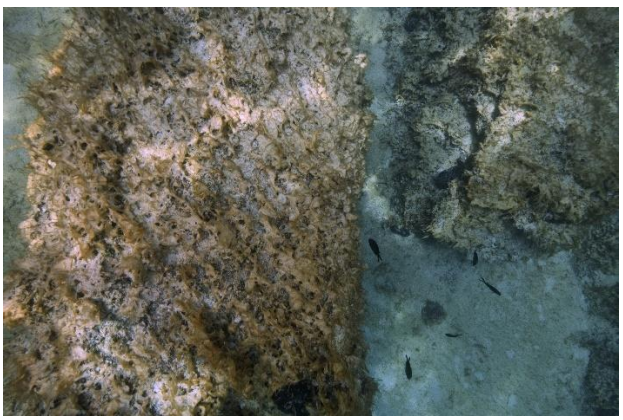

(b)

Figure 12. Comparison between the original image (a) and the one obtained after applying the colour correction model (b).

4.3 3D model reconstruction

Once the calibration parameters for Camera A and Camera B were extracted, the processing of the underwater acquisition has been conducted, using a pre-calibrated approach. An initial test has been performed by comparing two scenarios: one in which the cameras were constrained by their baseline distance and another in which no constraint was applied. When the cameras were constrained, 1312 stereo pairs have been successfully aligned, whereas only 534 stereo images have been aligned when no constraints have been applied. Also, as shown in Figure 13, the absence of constraints between the cameras resulted in a noticeably curved and distorted point cloud (bowl effect).

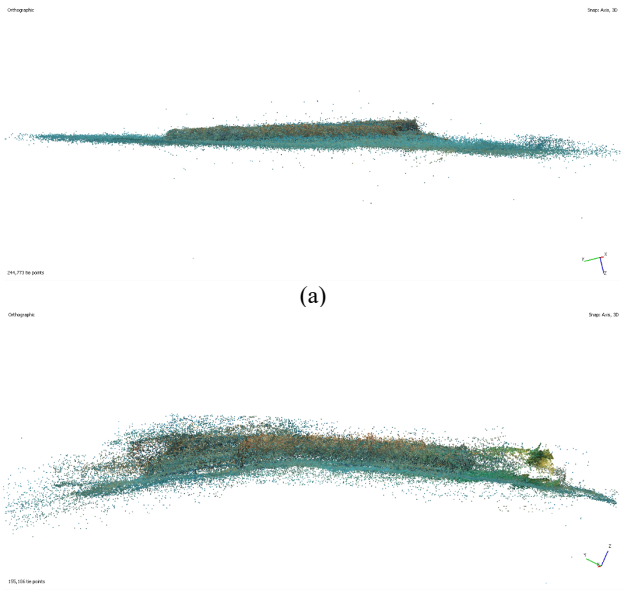

(a)

(b)

Figure 13. Point cloud obtained from the processing of the dataset with (a) and without (b) the baseline constraint.

Additionally, a comparison of the distortion plot residuals, which offer insights into the accuracy of the camera model and how well the estimated distortion parameters match the actual image observations, further confirmed this effect. The Root Mean Square (RMS) residual error, which reflects the average discrepancy between detected image points and their reprojected positions after applying the calibration model, was 3.83 pixels for the constrained configuration and 32.6 pixels for the unconstrained one.

As shown in Figure 14a, the residuals in the constrained setup are evenly spread and mostly within sub-pixel range, indicating a precise correction of lens distortion. The consistent radial pattern reflects a well-calibrated system, with slightly higher residuals at the edges. In contrast, the plot in Figure 14b displays large, irregular residuals, particularly at the image borders, highlighting poor calibration. The irregular distortion pattern and misaligned points suggest difficulty in modelling the camera geometry, likely due to the absence of the slave camera offset.

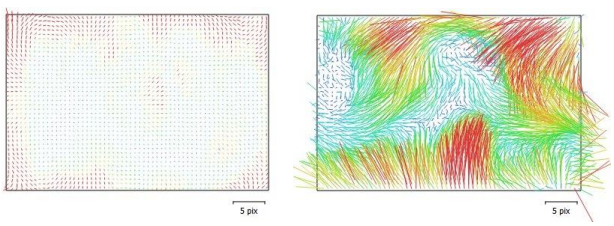

(a) (b)

Figure 14. Distortion plot of the residuals for restrained cameras (a) and unrestrained cameras (b).

A second and third reconstruction test were performed with the cameras constrained. In the second test, the calibration parameters (f, cx, cy, k1, k2, k3, p1, p2, b1, b2) were held fixed, whereas in the third test they were allowed to adjust. The third setup delivered improved reconstruction results: better alignment, lower total distortion, reduced residual errors (implying improved reprojection accuracy), and significantly decreased decentring distortion. However, this configuration also resulted in slightly higher radial distortion.

After assessing these configurations and selecting the best-performing one, the corrected and calibrated image set was used to generate the dense point cloud through multi-view stereo techniques in Agisoft Metashape. Thanks to the improved colour fidelity from the previous calibration and correction steps, feature matching and depth estimation were more robust, even in low-texture or shaded underwater areas (Figure 15).

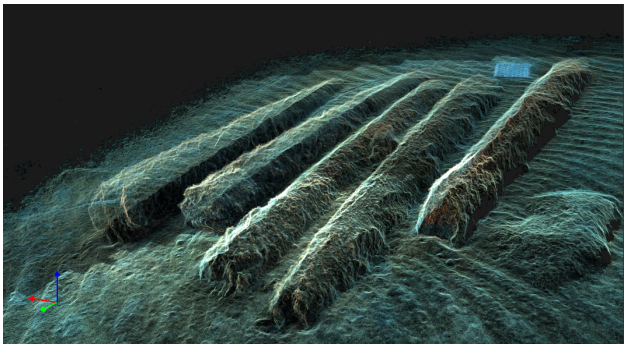

Figure 15. Screenshot of the obtained dense point cloud, visualised in the Nubigon software.

The dense cloud was then used to create a polygonal 3D mesh, textured using the radiometrically corrected images, preserving both geometric accuracy and chromatic realism. Finally, a high-resolution orthophoto (5mm/pixel) of the column structures has been extracted from the textured model. The orthophoto provides a metrically accurate and colour-corrected representation of the site, suitable for further archaeological analysis and documentation (Figure 16).

Integrating colour correction into the photogrammetric pipeline significantly improved the quality of the final 3D outputs, ensuring more faithful reconstructions in challenging underwater environments.

Figure 16. Final orthophoto derived from the 3D model of the five columns.

5. Results and Discussion

The implementation of the CRAB system for the underwater documentation of the Roman columns at Torre Chianca yielded promising results, both in terms of data quality and operational robustness. The acquisition campaign generated a dataset of 2632 high-resolution images (1316 stereoscopic pairs), which enabled the generation of a dense and metrically reliable 3D model of the site. The fixed baseline configuration, combined with pre-calibrated optical elements and controlled image overlap, contributed to a highly redundant photogrammetric block with stable geometric coherence across the entire surveyed area.

The most significant performance gain was observed when applying the fixed stereo baseline constraint during the Structure-from-Motion (SfM) processing stage. When the cameras have been treated as a rigid stereo pair, 1312 out of 1316 stereo couples have been successfully aligned, resulting in a complete and geometrically accurate point cloud. Conversely, omitting the baseline constraint led to a drastic reduction in image alignment (534 aligned stereoscopic pairs) and the generation of a deformed and non-metric point cloud, characterized by a pronounced curvature and concavity. This observation confirms the importance of applying rigid constraints in stereo acquisition systems, particularly in the absence of external georeferencing elements.

Distortion residual analysis further corroborated the superiority of the constrained configuration. The Root Mean Square (RMS) reprojection error was limited to 3.83 pixels with constrained cameras, compared to 32.6 pixels in the unconstrained scenario. The residuals exhibited a uniform radial distribution, indicating effective distortion compensation and validating the pre-survey camera calibration procedure. In contrast, the unconstrained configuration produced erratic residual patterns, with significant deviations at the image periphery, likely due to the algorithm's inability to model the stereo geometry without fixed internal constraints.

Additional tests comparing fixed versus dynamic internal parameter optimisation revealed a trade-off between model flexibility and metric consistency. When keeping the calibration parameters locked, the resulting model was stable but showed slightly higher residuals and less adaptability to scene-specific lens behaviour. Allowing partial recalibration led to improved fit and lower decentring distortion but introduced increased radial distortion, underscoring the need for a balanced calibration strategy tailored to the specific acquisition geometry and optical setup.

The integration of the CRAB system in an active archaeological context also demonstrated its operational viability. The stereo rig proved to be manageable by a team of two divers and compatible with standard excavation protocols. The visibility conditions during the campaign, enhanced by the excavation team's prior removal of marine sediment, enabled the full documentation of the exposed marble surfaces, improving the level of detail and completeness of the reconstruction. The resulting model provides not only a high-fidelity geometric record but also valuable information for assessing the conservation state and spatial distribution of the architectural elements.

Nevertheless, some limitations emerged. The system's effectiveness is influenced by environmental factors such as water turbidity, light attenuation, and biofouling, which can degrade image quality and affect colour correction performance. The absence of an integrated georeferencing solution (e.g., GNSS-inertial navigation) restricts the system's ability to deliver absolute positioning, limiting its use in large-scale or deep-sea scenarios without external control points

6. Conclusions

This study validates the CRAB (Calibrated Rig for Aquatic photogrammetric Bicamera system) as a robust, high-resolution tool for the metric documentation of submerged cultural heritage. Through its stereo acquisition configuration, optical pre-calibration, and structured acquisition methodology, CRAB effectively addresses several of the principal limitations of underwater photogrammetric workflows, including geometric distortion, lack of ground control, and image misalignment.

The field deployment at Torre Chianca demonstrated that the system can produce metrically accurate 3D reconstructions under real operational conditions. Imposing a fixed baseline during image processing proved essential to ensuring internal consistency and minimizing model deformation. The experimental results underline the necessity of precise calibration and acquisition planning when operating in optically complex environments such as shallow marine settings.

The CRAB system's modularity and portability also make it highly adaptable for various underwater contexts beyond the case study presented here. Potential applications include the documentation of shipwrecks, submerged architectural remains, underwater sculptures, and even modern infrastructure inspections. Furthermore, the integration of colour correction directly into the 3D reconstruction pipeline enhances the system's utility for creating visually accurate, high-quality models that can serve both scientific analysis and public dissemination.

From an operational perspective, the portability and modularity of the CRAB system make it suitable for integration into multidisciplinary field campaigns, facilitating real-time coordination between geomatics specialists and archaeological teams. Its successful application within an underwater archaeological site emphasises its potential as a documentation tool not only for post-excavation analysis but also for in situ monitoring and stratigraphic interpretation.

Future developments will focus on enhancing radiometric calibration strategies, integrating inertial navigation systems for improved georeferencing, and adapting the system for use in more challenging underwater conditions, such as low-visibility or greater depths.

Acknowledgments

The authors would like to thank the underwater archaeological team from the Università del Salento, with special thanks to Professor Rita Auriemma, Luigi Coluccia, Angelo Colucci, Cristiano Alfonso, and Giuliana Marfeo, for their invaluable support and presence during the data acquisition phase. Thanks to Pasquale Genzano from Aquateks and to the other colleagues of the Politecnico di Torino Geomatics team Nives Grasso, Alessio Martino, and Francesca Matrone, for their help during the testing and acquisition phases.

Many thanks also to the WEEE Open student team from Politecnico di Torino for their work on optimizing the hardware and software components of CRAB, and to Gianluca Dara from the PoliTo Interdepartmental Centre for Service Robotics (PIC4SeR) for his help with the system's electrical components.

This publication is part of the project PNRR-NGEU which has received funding from the MUR – DM 351/2022.

Also, the CRAB system has been developed under the ARCHIM3DES and the POSEIDON projects.

Poseidon is a research project of Italian national relevance initiative "Italia Domani - Piano Nazionale di Ripresa e Resilienza" (PNRR) funded by the European Commission - Next Generation EU.

Finanziato dall'Unione europea NextGenerationEU | Ministero dell'Università e della Ricerca | Italiadomani

References

Auriemma, R., Calantropio, A., Chiabrando, F., Coluccia, L., Rugge, M., D'Ambrosio, P., Buccolieri, M. and Picciolo, A., 2021. Underwater archaeological surveys in Salento waters: results and methods. *FOG-Freiberg Online Geoscience*, *58*.

Balletti, C., Beltrame, C., Costa, E., Guerra, F. and Vernier, P., 2015. Underwater photogrammetry and 3D reconstruction of marble cargos shipwreck. *International Archives of the Photogrammetry, Remote Sensing and Spatial Information Sciences*, *40*, pp.7-13.

Calantropio, A., Chiabrando, F. and Auriemma, R., 2021. Photogrammetric underwater and UAS surveys of archaeological sites: The case study of the roman shipwreck of Torre Santa Sabina. *The International Archives of the Photogrammetry, Remote Sensing and Spatial Information Sciences*, *43*, pp.643-650.

Calantropio, A. and Chiabrando, F., 2024. Underwater cultural heritage documentation using photogrammetry. *Journal of Marine Science and Engineering*, *12*(3), p.413.

Menna, F., Nocerino, E., Fassi, F. and Remondino, F., 2016. Geometric and optic characterization of a hemispherical dome port for underwater photogrammetry. *Sensors*, *16*(1), p.48.

Ricca, M., Alexandrakis, G., Bonazza, A., Bruno, F., Davidde Petriaggi, B., Elkin, D., Lagudi, A., Nicolas, S., Novák, M., Papatheodorou, G. and Prieto, J., 2020. A sustainable approach for the management and valorization of underwater cultural heritage: new perspectives from the TECTONIC project. *Sustainability*, *12*(12), p.5000.

She, M., Song, Y., Mohrmann, J. and Köser, K., 2019. Adjustment and calibration of dome port camera systems for underwater vision. In *Pattern Recognition: 41st DAGM German Conference, DAGM GCPR 2019, Dortmund, Germany, September 10–13, 2019, Proceedings 41* (pp. 79-92). Springer International Publishing.

Schettini, R. and Corchs, S., 2010. Underwater image processing: state of the art of restoration and image enhancement methods. *EURASIP journal on advances in signal processing*, *2010*, pp.1-14.

She, M., Nakath, D., Song, Y. and Köser, K., 2022. Refractive geometry for underwater domes. *ISPRS Journal of Photogrammetry and Remote Sensing*, *183*, pp.525-540.

Violante, C., 2018. A geophysical approach to the fruition and protection of underwater cultural landscapes. Examples from the Bay of Napoli, southern Italy. *La Baia di Napoli. Strategie per la conservazione e la fruizione del paesaggio culturale*, pp.64-71..